Available online at www.sciencedirect.com
SCIENCE DIRECT®
Journal of Power Sources 140 (2005) 203–210
JOURNAL OF POWER SOURCES
www.elsevier.com/locate/jpowsour

Performance of experimental carbon blacks in aqueous supercapacitors

Mathieu Toupin[a], Daniel Bélanger[a,1], Ian R. Hill[b,*], David Quinn[c]

[a] *Département de Chimie, Université du Québec à Montréal, Case Postale 8888, Succursale Centre-Ville, Montréal, Québec, Canada H3C 3P8*
[b] *Institute for Chemical Process and Environmental Technology, National Research Council of Canada, Ottawa, Ont., Canada K1A 0R6*
[c] *Department of Chemistry and Chemical Engineering, Royal Military College of Canada, Kingston, Ont., Canada K7K 5L0*

Received 16 July 2004; accepted 17 August 2004
Available online 6 October 2004

Abstract

Four samples of carbon black were synthesised for use in aqueous supercapacitors. They were designed to have different surface areas and pore size distributions. The objectives were to identify the attributes that are necessary to obtain a high specific capacitance and to attempt to correlate different physical characteristics of the carbon electrodes with their capacitance. A fifth carbon was obtained from another laboratory for comparison. Carbon electrodes were analysed using both acidic and alkaline electrolytes. Their capacitance was measured at room temperature and at −40 °C, using slow sweep cyclic voltammetry. Electrochemical impedance spectroscopy was also performed on the carbon electrodes using the same electrolytes and temperatures. The results from these measurements are discussed in terms of the surface areas and pore size distributions of the samples, which were measured using the BET technique.

Keywords: Supercapacitor; Electrochemical capacitor; Specific capacitance; Carbon; Aqueous electrolyte

1. Introduction

Electrochemical supercapacitors using carbon as the active electrode material have been investigated for almost 30 years, but there has recently been increasing interest due to the need for high power energy sources in portable electronics and for electric vehicles. A wide variety of carbon materials have been prepared and tested and those include: carbon blacks, glassy carbon, activated carbons, carbon microbeads, fibres, cloths, aerogels and nanotubes [1–14].

The mechanism of energy storage in carbon-based electrochemical capacitors primarily involves charge separation at the carbon/electrolyte interface, leading to a double layer capacitance [1]. In addition, the presence of electroactive groups at the carbon surface can also lead to a capacitance known as pseudocapacitance; the capacitance associated with the redox processes of these surface groups can be of the order of 5–10% of the double layer value. The conventional approach for the preparation of the carbons commonly focuses on obtaining high surface area and highly porous materials. This approach can produce capacitance values greater than 100 Fg^{-1} when the surface area is in the order of 1000–2000 $m^2\,g^{-1}$. The porous structure of these materials can be described using three widely varying sizes: micropores (<2 nm), meso-pores (between 2 and 50 nm) and macropores (>50 nm) [7]. It is now fairly well established that most of the capacitance is generated at the surface of micro-pores, although a significant fraction of the micro-pores may not be electrochemically accessible [8,9]. Pore accessibility will be dependent on the nature of the electrolyte, such as the sizes of the ionic species and the solvent molecules, plus the nature of the surface groups on the carbon.

The carbon samples used in this work were produced such that they had different pore size distributions. The intent of this was to try and establish the effect that pore size had on both the capacitance and the cycling rate. For most applications, electrochemical capacitors are used at room

* Corresponding author. Tel.: +1 613 998 6814; fax: +1 613 991 2384.
E-mail addresses: belanger.daniel@uqam.ca (D. Bélanger), ian.hill@nrc-cnrc.gc.ca (I.R. Hill).
[1] Tel.: +1 514 987 3000x3909; fax: +1 514 987 4054.

0378-7753/$ – see front matter © 2004 Elsevier B.V. All rights reserved.
doi:10.1016/j.jpowsour.2004.08.014

temperature; however, some applications may require operation in the range of −20° and −50 °C. Unfortunately, there have been very few studies on the performance of carbon-based supercapacitors at low temperatures [10]. Therefore, another objective of the present work was to evaluate the performance of the carbon-composite electrodes at low temperatures.

2. Experimental

The carbon powders used in this work were prepared at the Royal Military College of Canada (A, B, C and E) and at the Institute for Hydrogen Research at the Université du Québec à Trois-Rivières (D). Sample A was prepared from ground peach stone, treated with phosphoric acid at 500 °C. Sample B was furfuryl resin that had been acid polymerised in the presence of a pore former. The resin was then pyrolised at 750 °C. The pore former was used to produce large numbers of meso- and macro-pores. Sample C was saran copolymer, pyrolised at 750 °C to produce large numbers of micro-pores. The preparation of sample D was proprietary. Sample E was ground peach stone that was pyrolised at 750 °C then treated with KOH at 850 °C with the aim of producing a range of micro- and meso-pores. Infrared spectra of the carbon samples in KBr pellets were measured using a Perkin-Elmer System 2000.

Composite electrodes were prepared by mixing the carbon samples with graphite (Alfa Aesar, conducting grade, −200 mesh), acetylene black (Alfa Aesar, >99.9%, surface area = 80 $m^2 g^{-1}$), and polytetrafluoroethylene powder (ratios: 90:5:0.1:5, respectively), using methanol to wet the mixture. The paste was then cold-rolled into 100 μm thick films. Typical loadings of the carbon active material were 4–5 mg cm^{-2}. Pieces of film, typically 7 mm × 6 mm size and weighing around 1 mg, were then pressed at 900 MPa onto a titanium or stainless steel mesh. The mesh was tabbed using copper wire that was insulated from the electrolyte using epoxy resin.

Electrochemical tests were performed using a Solartron 1470 battery tester operated under Corrware II software (Scribner Associates). The electrochemical impedance measurement apparatus consisted of a Solartron 1287 potentiostat–galvanostat coupled to a Solartron 1255 frequency response analyser. All of the samples were tested in both acid and alkali solutions (7 M H_2SO_4 and 7 M KOH), at both room temperature and −40 °C. Platinum gauze was used for the counter electrode and the reference electrodes were Hg/Hg_2SO_4 (saturated K_2SO_4) or Ag/AgCl (saturated NaCl). A dry ice–ethylene glycol bath was used for the experiments at −40 °C.

The specific capacitance C (Fg^{-1}) of a given composite electrode was determined by integrating the cyclic voltammogram to obtain the voltammetric charge (Q), and subsequently dividing this charge by the mass of the carbon active material (m) and the width of the potential window (ΔE) ($C = Q/(m\Delta E)$). The contribution that acetylene black (specific capacitance: 12 Fg^{-1}) made to the capacitance was neglected because of the small amount present. Nitrogen sorption measurements at 77 K were performed using a Micromeritic Flowsorb II/2300 surface area analyser to evaluate the BET surface area and also the pore size distribution of both the carbon powders and the composite electrodes. Graphite has a very low BET surface area (around 2 $m^2 g^{-1}$) compared with the carbon black samples, so its surface area was neglected.

3. Results and discussion

3.1. Physical characterisation

The specific surface areas and pore volumes obtained from BET measurements of the carbon samples are listed in Table 1, along with the average pore diameters. The measurements were made on the composite electrodes and the values can be seen to vary widely between the samples. The pore volumes and pore areas of the samples are plotted in Fig. 1a and b for comparison. A line has been added at 2 nm in the figures, to signify the rough boundary between micro-pores and meso-pores. Sample E can be seen to have both the highest pore area and pore volume: the sample also has a fairly even mixture of micro-pores and meso-pores. Sample D is similar to sample E, but it has a lower pore area and pore volume in the 2 nm region; however, sample D has a significantly higher pore volume in the 10–50 nm region, which it was believed could increase the access of electrolyte to the micro-pores and cause this sample to have a higher capacitance than sample E. The pore area of samples A, B and C can be seen to mainly derive from micro-pores. Samples A and C are similar but the pore volume of C has a maximum around 1.7 nm, so the average pore size is slightly larger. Sample B has a low surface area but a high proportion of large meso-pores and macro-pores, giving it the highest average pore size out of all the samples. This sample was expected to show whether large meso-pores were important for the electrolyte to penetrate the micro-pores. It was anticipated that sample B could have a higher capacitance than samples A and C because of its higher average pore size, even though sample B does have a significantly lower surface area. Fig. 1c compares the pore volumes of all five carbon samples with their corresponding micro-pore volumes. Samples D and E clearly have much higher micro-pore and meso-pore volumes

Table 1
Surface area and pore volumes of the carbon samples, obtained from the composite electrodes

Carbon sample	Surface area ($m^2 g^{-1}$)	Pore volume ($cm^3 g^{-1}$)	Average pore diameter (nm)
A	563	0.25	1.4
B	436	0.34	2.8
C	657	0.30	1.8
D	2100	1.48	2.2
E	2692	1.65	2.0

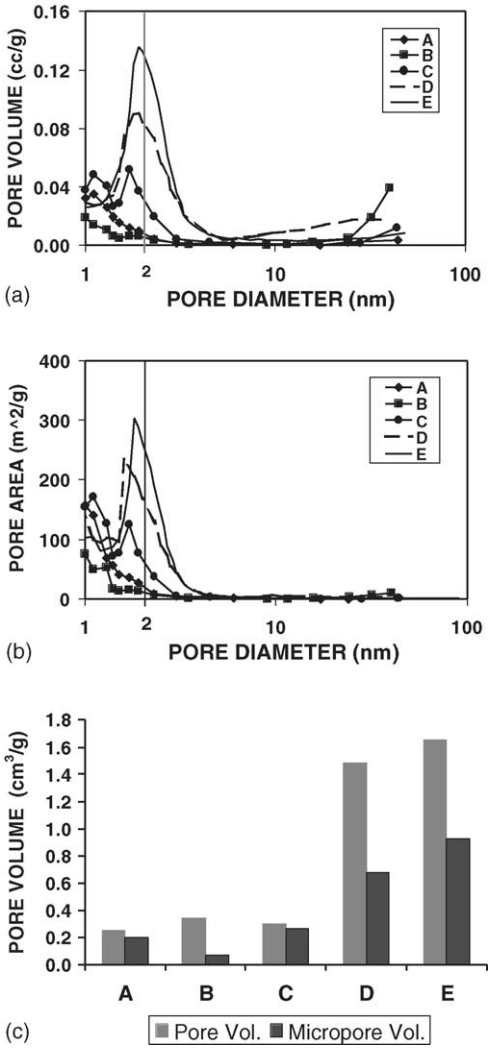

Fig. 1. A comparison of the pore size distribution of the carbon samples: (a) pore volume and (b) pore area. A line has been added at 2 nm, which serves as a rough division between micro-pores and meso-pores. (c) Comparison of the pore and micro-pore volumes of the carbons.

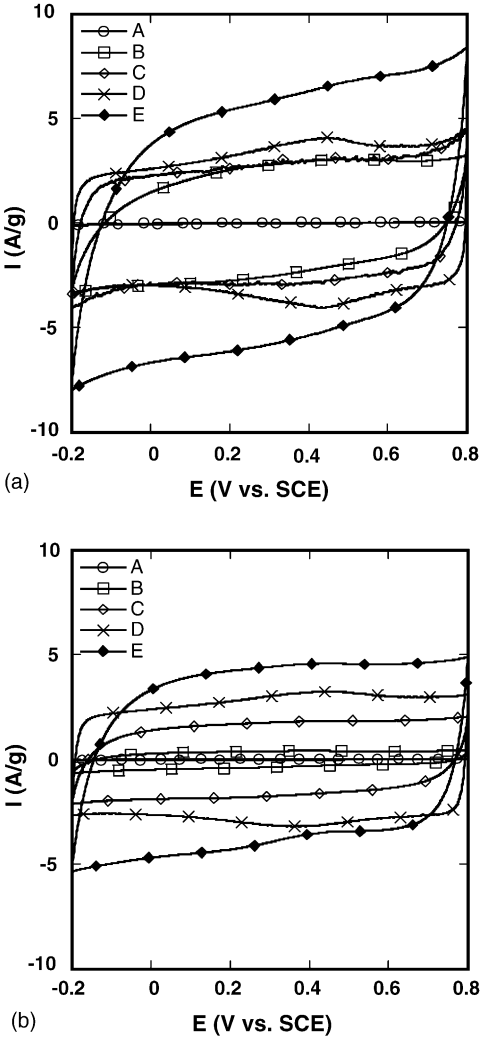

Fig. 2. (a) Cyclic voltammograms of the carbon samples, in 7 M H_2SO_4 at room temperature, using a scan rate of 20 mV s^{-1}. (b) Cyclic voltammograms of the carbon samples, in 7 M H_2SO_4 at −40 °C, using a scan rate of 20 mV s^{-1}.

than the other samples and were expected to yield a high capacitance. The micro-pores provide a high surface area and the meso-pores were expected to allow good electrolyte penetration.

3.2. Electrochemical characterisation

3.2.1. Cyclic voltammetry in H_2SO_4 at room temperature and −40 °C

Fig. 2a shows representative cyclic voltammograms (CVs) recorded at room temperature in 7 M sulphuric acid, using a scan rate of 20 mV s^{-1}. The CVs of samples C and D are almost rectangular, as expected for materials characterised by a capacitive behaviour. Samples B and E are less ideal, with a sloping profile, while sample A showed very poor capacitive behaviour. Sample A had been made using the same starting material as sample E, which yielded the highest capacitance. The reason that sample A was so poor was because it contained organic residue due to insufficient heating during synthesis, showing how important it is to have complete reaction. The infrared spectrum of sample A exhibited a band arising from carbonyl groups (1695 cm^{-1}) that was not present in any of the other samples, and also strong bands arising from quinone (1585 cm^{-1}) and C–O species (1195 cm^{-1}) that were not present in sample E. The latter sample had been heated at a higher temperature than sample A and treated with KOH. Although sample A did not have the lowest surface area out of the carbon samples, it had a much higher resistance than the others, making it useless for the present application. The presence of redox waves, clearly noticeable for sample D at about 0.45 V, are attributed to the redox reactions of electroactive surface functional groups such as [4]:

$$\text{phenolic} \quad \rangle\text{C–OH} \leftrightarrow \text{C=O} + \text{H}^+ + e^- \tag{1}$$

$$\text{carboxylic} \quad \text{–COOH} \leftrightarrow \text{–COO} + \text{H}^+ + e^- \tag{2}$$

ketone $\gtrless C{=}O + e^- \leftrightarrow C{-}O^-$ (3)

The pseudocapacitance provided by these groups should be beneficial, but they are also subject to a higher self-discharge rate than the capacitance derived from the double layer [1]. Infrared spectra of the carbon samples showed that sample D contained appreciable amounts of quinone groups (1570 cm^{-1}) while sample E did not, in agreement with the presence of redox waves in the cyclic voltammogram of sample D. Fig. 2b shows the corresponding cyclic voltammograms measured at −40 °C. Here, the capacitance of the samples was generally lower but the plots are more ideal. The samples were all also charged and discharged using a constant current of 250 mA g^{-1} and the variation of the potential with time was close to linear, as expected for capacitance (this data is not shown, for brevity).

3.2.2. Cyclic voltammetry in KOH at room temperature and −40 °C

Fig. 3 shows representative CVs for the carbon samples in 7 M KOH, both at room temperature (a) and at −40 °C (b). A strong polarisation is seen for all of the samples and sample A again displays poor capacitive behaviour. The CVs obtained at room temperature show an increase in current at the positive potential limit, which is absent at low temperature. This is the onset of oxidation of carbon to carbonate [11], which should be avoided. When these samples were charged at room temperature using a constant current of 250 mA g^{-1}, the potential increased almost linearly up to +0.1 V and then the rate slowed considerably, confirming that the predominant behaviour above 0.1 V was faradaic. However, linear behaviour was obtained up to +0.2 V at −40 °C.

3.2.3. Capacitance in acidic and alkaline electrolytes

The specific capacitances derived from the CVs are recorded in Table 2. Sample E had the highest capacitance (Fg^{-1}) in all cases, which was much higher than the other samples. The capacitance values for this sample ranged from 213 to 279 Fg^{-1}, according to the experimental conditions (electrolyte and temperature). The other high surface area sample, *D*, gave values of about 150 Fg^{-1} at room temperature. The two high surface area carbons lost a lower percentage of their capacitance upon cooling to −40 °C than the other samples; nevertheless the capacitance was 25% (D) and 10%

Table 2
Specific capacitance of the carbon samples under different experimental conditions

Carbon sample	Capacitance in H_2SO_4 Fg^{-1} ($\mu F\,cm^{-2}$)		Capacitance in KOH Fg^{-1} ($\mu F\,cm^{-2}$)	
	RT	−40 °C	RT	−40 °C
A	2	2	28	27
B	127 (29.1)	19 (4.3)	126 (28.8)	68 (15.5)
C	134 (20.3)	49 (7.4)	154 (23.4)	45 (6.8)
D	164 (7.8)	140 (6.6)	148 (7.0)	106 (5.0)
E	279 (10.3)	213 (7.9)	267 (9.9)	237 (8.8)

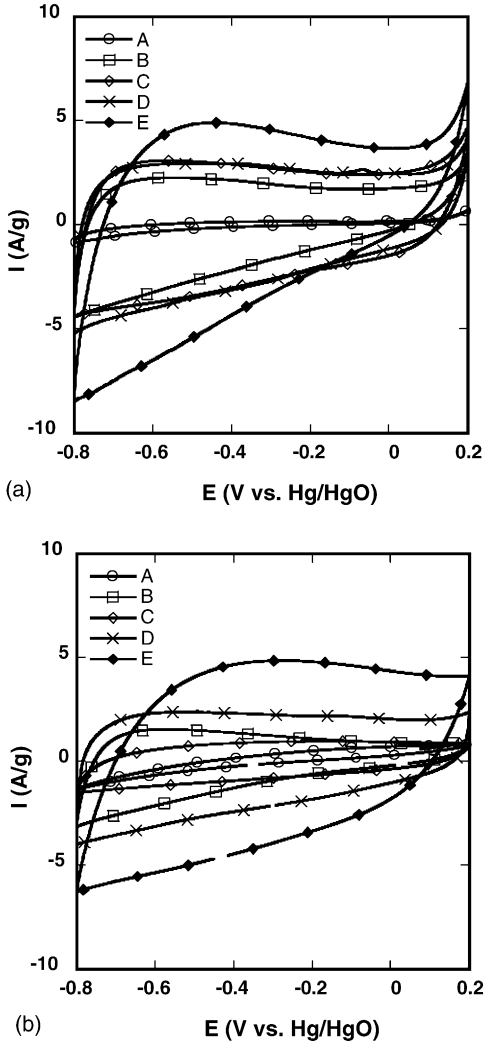

Fig. 3. (a) Cyclic voltammograms of the carbon samples, in 7 M KOH at room temperature, using a scan rate of 20 mV s^{-1}. (b) Cyclic voltammograms of the carbon samples, in 7 M KOH at −40 °C, using a scan rate of 20 mV s^{-1}.

(E) lower than at room temperature. A similar decrease in capacitance has recently been reported for carbon electrodes tested between 25 and −18 °C in non-aqueous electrolyte [10]. The specific capacitance of samples B and C decreased significantly between room temperature and −40 °C: this behaviour will be discussed below.

3.3. Relationship between the specific capacitance and BET data

Fig. 4 compares the specific capacitance, obtained from the carbons in acid and alkali at room temperature plus at −40 °C, with their pore and micro-pore areas. Ignoring sample A, there is a general trend of increasing capacitance with surface area. However, there clearly cannot be a simple relationship between capacitance and surface area, because the capacitance varies with temperature. The correlation between

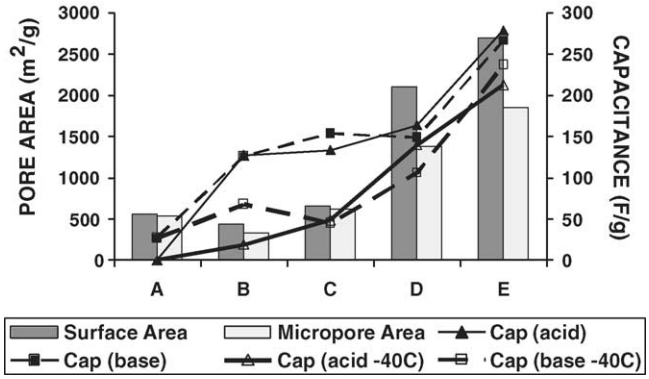

Fig. 4. A comparison of the capacitance (evaluated by cyclic voltammetry) with both the pore and micro-pore areas of the carbon samples.

capacitance and micro-pore area is slightly better than that with the total pore area. The absence of a simple correlation has previously been reported [7]. Other attempts to correlate the capacitance with a physical property of the electrodes have considered micro-pore and meso-pore volumes [8,12]. Despite some success with this approach, the correlation did not hold in all cases. In the present work, there was a rough correlation between capacitance at −40 °C and micro-pore volume, which was at a similar level to the correlation with micro-pore area. However, there was a definite lack of correlation between the capacitance at room temperature and micro-pore volume and also between the capacitance and total pore volume or micro-pore area.

The observation of a strong temperature effect provides some insight into other experimental factors that may contribute to the capacitance of carbon. One of these factors is the identification of those small pores that do not contribute to the capacitance because they are not electrochemically accessible [12]. For example, Fig. 4 demonstrates that the capacitance of samples B, C and D is similar in alkaline and acidic media at room temperature despite the fact that the meso- and micro-pore areas of D are much larger. This indicates that a significant proportion of the micro-pore surface area of sample D is probably not electrochemically accessible: the capacitance data in Table 2 shows that sample D has the lowest value in terms of area (7.8 μF cm^{-2}). The pore volume data of Fig. 1a shows that sample D has a high level of pore volume derived from large meso-pores, which was expected to assist in the wetting of the micro-pores. This does not seem to have occurred, or there must be another reason for the lower than expected capacitance of sample D. In Fig. 4, it can be seen that samples B and C suffer a much higher proportionate loss in capacitance at −40 °C than D and E do. This implies that the high meso-pore volumes of sample D and E could be important at −40 °C, along with other factors such as conductivity and viscosity.

Table 2 shows that samples B and C had a higher capacitance per unit area than samples D and E. Sample C had a very high number of micro-pores and few meso-pores, but its micro-pores were apparently wetted proportionately more than those in samples D and E. Therefore, the problem appears to be that the very high volume of small micro-pores and meso-pores in samples D and E are difficult to fully wet, whether large meso-pores are present or not, possibly because of trapped air. Alternatively, because of the extensive network of micro-pores in samples D and E, there could be a loss of electrical conductivity in the region of some of the micro-pores. These aspects require further investigation. The higher proportionate fall in capacity of samples B and C at low temperature, compared with samples D and E, is not understood at this time.

Table 3
Conductivity and viscosity of 7 M H_2SO_4 and 7 M KOH solutions

	7 M H_2SO_4		7 M KOH	
	RT	−40 °C	RT	−40 °C
Conductivity, S cm^{-1}	0.585	0.11	0.65	0.06
Viscosity, cP	3.4	29	2	36

Table 3 shows the conductivity and viscosity changes of the electrolytes between RT and −40 °C. The changes indicate that diffusivity of the ions will be hindered at low temperature and consequently a larger fraction of the very small pores are likely to be inactive. From Table 3, the changes in conductivity and viscosity of 7 M KOH are much higher than those of 7 M H_2SO_4. This implies that there could be a larger drop in capacitance in the alkali media at low temperature compared with the acid. However, Fig. 4 shows that this was not the case in our experiments. Therefore, the temperature dependence of the capacitance has more complex origins.

3.4. Electrochemical impedance spectroscopy

3.4.1. Nyquist plots

Figs. 5 and 6 show Nyquist plots for the carbon samples in 7 M H_2SO_4. Fig. 5 shows the complete range that was swept (0.01 Hz to 60 kHz), while Fig. 6 is an expansion of the high frequency parts of the spectra. The Nyquist plots of sample A are not included since they displayed a very large semicircle and no vertical tail at low frequency, which is consistent with the lack of capacitance obtained for this sample. Similar electrochemical impedance behaviour to that of sample A has also been reported for a carbon xerogel that was carbonised at 600 °C. The behaviour was ascribed to incomplete conversion into electrically conducting carbon [7], which was also the case for sample A here.

The Nyquist plots are characterized by a semi-circle at high frequency and a sharp increase in the imaginary part of the impedance at lower frequency. The high frequency intercept on the Z' axis represents the sum of the resistances arising from the electrolyte, the intrinsic resistance of the carbon active material, and the contact resistance between the active material and the current collector (R_s). Fig. 6 shows that samples B and D have significantly higher R_s values than the other two samples. Samples B and D also have the highest number of large meso-pores, so the R_s values probably

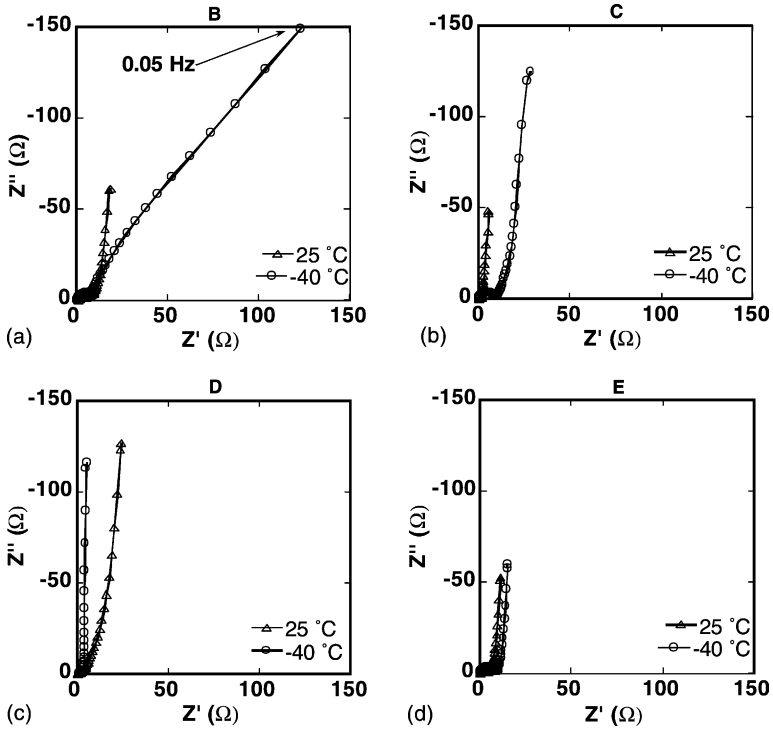

Fig. 5. Nyquist plots for the carbon-composite electrodes in 7 M H_2SO_4: (a) B; (b) C; (c) D; and (d) E.

reflect an increased intrinsic resistance of the carbon because of the large pores. The semi-circle is associated with faradaic reactions (pseudocapacitance) and also the porous structure of the carbons [8]. The diameter of the semicircle is referred to as the polarisation resistance, R_P. It should be noted that other explanations related to the resistance of the current collector, and presumably not associated to the porous nature of the electrode, have also been given to explain the pres-

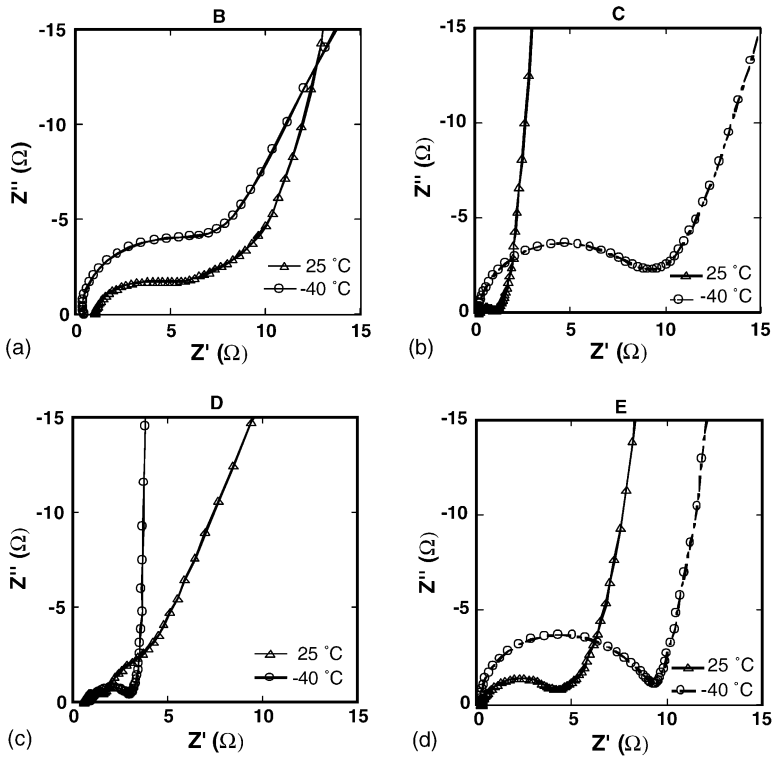

Fig. 6. Enlarged sections of the Nyquist plots from Fig. 5 (7 M H_2SO_4): (a) B; (b) C; (c) D; and (d) E.

ence of the semicircle [15]. The low frequency data should yield a vertical line for an ideal capacitor. Deviation from the ideal 90° is associated with a broad pore size distribution, which has been explained by the fact that penetration of the ac signal will depend on the size of the pores: penetration will be deep for macro-pores and shallow for micro-pores [8]. It should be noted that only the Nyquist plot of sample B at −40 °C does not show a near-vertical line at low frequency. This sample has a broad pore size distribution, with the main pore sizes being in the micro-pore and large meso-pore regions.

The polarisation resistance (R_P) and the low frequency resistance (R_{LF}) were measured from the impedance plots. The former was obtained from the diameter of the semi-circle, while R_{LF} was determined by extrapolation of the capacitive line to the real impedance axis. The R_{LF} values represent the overall resistance of the electrochemical cell so, obviously, should be as small as possible to minimize the energy losses during cycling.

No simple correlation was found between the R_P or R_{LF} values of the carbons and properties such as the capacitance or pore volume. The relatively large R_P value of sample E at room temperature (4 Ω) in comparison with sample D (0.5 Ω) is interesting because sample E also exhibited the highest capacitance. The large R_P value should not be associated with the pseudocapacitive redox reaction because Fig. 2 shows that there was no peak observed around 0.4 V for this sample, whilst there was for sample D. Therefore, the large R_P value is believed to reflect higher penetration of the electrolyte into the micro-pores of sample E, as indicated by the higher value of the specific capacitance (μF cm^{-2}) of sample E in Table 2. The R_P value is high because the mass transfer rate of ions into the micro-pores is lower than that into meso-pores [16]. However, the apparently higher penetration of electrolyte into the micro-pores of sample E in comparison with sample D is not understood, because sample D contains a high concentration of large macro-pores which are meant to assist wetting of the micro-pores. In addition, sample D contains appreciable amounts of quinone groups, which were expected to enhance the wettability of the carbon surface, although these groups may not be present inside the micro-pores.

The impedance spectra were also measured in 7 M KOH. The spectra looked similar in shape to those obtained in 7 M H_2SO_4, except that the R_P and R_{LF} values were approximately double the size and the low frequency tails tended to be less vertical. The data imply that KOH may not sustain as high cycling rates as H_2SO_4, as will be discussed in the next section. When going from room temperature to −40 °C, sample C exhibited the largest increase in R_P in both acid and alkali. This sample also had the largest percentage decrease in capacitance for acid and alkali, when the temperature was reduced to −40 °C. Sample C had the highest concentration of small micro-pores, so it is possible

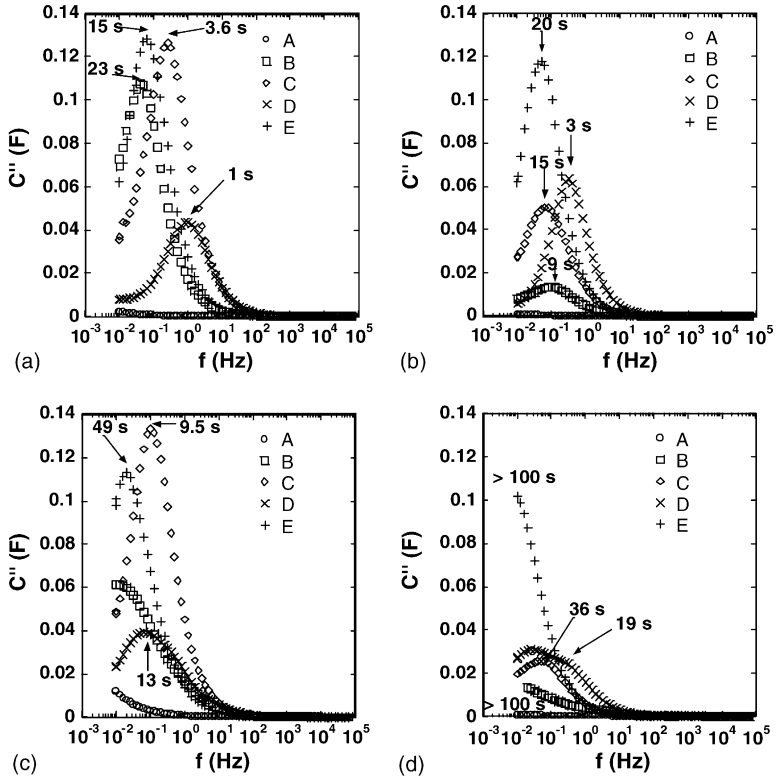

Fig. 7. Bode plots of the imaginary capacitance as a function of the frequency for carbon-composite electrodes in: (a) 7 M H_2SO_4 at room temperature; (b) 7 M H_2SO_4 at −40 °C; (c) 7 M KOH at room temperature and (d) 7 M KOH at −40 °C.

that these are less accessible at −40 °C and cause the large increase in R_P, plus the large fall in capacitance.

3.4.2. Bode plots

A recent report has demonstrated that a Bode plot of the imaginary part of the capacitance as a function of frequency is useful for gaining insight into the discharge time of the carbon material [14]. The minimum discharge time for a carbon electrode is an important factor, which is inversely related to the power that can be delivered during discharging. Such plots are shown in Fig. 7. For most of the carbons, a maximum is observed at a characteristic frequency. The reciprocal of this frequency represents the minimum time (τ) that could be used for the charge or discharge of the electrode material while maintaining a good capacitive behaviour [14].

The Bode plots of Fig. 7 show that the frequency of the imaginary capacitance maximum decreases when the temperature is lowered to −40 °C and that it is also lower in alkali than in acid. The smaller τ values found in the acidic electrolyte imply that higher power discharging should be obtained in acid. This is consistent with the lower R_{LF} values that were obtained from the Nyquist plots for acidic solution. The observation of a longer time constant for sample E relative to D implies that sample D should have better high rate performance than E, even though it has lower capacitance. This is consistent with sample D having a higher number of large meso-pores than sample E, which allows "connection" between the micro-pore areas. The data were further analysed by comparing the τ values with the pore volumes and capacitance, but no correlation was evident.

4. Conclusions

The carbon samples investigated in this work were found, on average, to display similar capacitance in 7 M H_2SO_4 and 7 M KOH. The capacitance obtained from sample E at room temperature, using a slow cyclic voltammetric sweep, was 270 Fg^{-1}, which is a particularly high value. This sample had been prepared from ground peach stones that were pyrolised and treated with KOH especially to produce a range of micro-pores and meso-pores. The capacitance obtained at −40 °C was significantly lower than that obtained at room temperature, plus the fall in capacitance varied widely between the samples. The fall in capacitance with temperature decrease was significant for samples B and C and their values (approximately 50 Fg^{-1} at −40 °C) are much too low for practical use in a capacitor. On the other hand, samples D and E yielded capacitances of approximately 120 and 220 Fg^{-1} at −40 °C, respectively, and should be good candidates for use in electrochemical capacitors for low temperature operation.

No simple correlation was found between the capacitance of the carbons and either the surface area or the pore size distribution. Our data suggested that a significant fraction of the micro-pores are not electrochemically accessible. This could be due to the relative sizes of the pores and the ionic species that are involved in the double layer capacitance. It is apparent that several factors influence the capacitance of carbonaceous materials. Analysis of the impedance data, using Bode plots, provided some insight into the rate capability of these carbon materials in an electrochemical capacitor. The results indicated that, although the presence of a high concentration of large meso-pores and macro-pores did not appear to affect the specific capacitance, they should enhance the rate capability.

Acknowledgements

The authors would like to thank Stephen Argue of the National Research Council for making the BET measurements on the carbon samples. Mathieu Toupin would like to thank Defence Research and Development Canada for financial support. This work was funded by contract W7707-010273/001/HAL from the Department of National Defence (Canada).

References

[1] B.E. Conway, Electrochemical Supercapacitors Scientific Fundamentals and Technological Applications, Kluwer Academic/Plenum Press, New York, 1999.
[2] R. Kötz, M. Carlen, Electrochim. Acta 45 (2000) 2483.
[3] A.J. Burke, J. Power Sources 91 (2000) 37.
[4] E. Frackowiak, F. Béguin, Carbon 39 (2001) 937.
[5] D. Qu, H. Shi, J. Power Sources 74 (1998) 99.
[6] D. Qu, J. Power Sources 102 (2001) 270.
[7] H. Shi, Electrochim. Acta 41 (1996) 1633.
[8] J. Gamby, P.L. Taberna, P. Simon, J.F. Fauvarque, M. Chesneau, J. Power Sources 101 (2001) 109.
[9] C. Lin, B.N. Popov, H.J. Ploehn, J. Electrochem. Soc. 149 (2002) 167.
[10] L. Bonnefoi, P. Simon, J.F. Fauvarque, C. Sarrazin, J.F. Sarrau, A. Dugast, J. Power Sources 80 (1999) 149.
[11] D. Tryk, W. Aldred, E. Yeager, in: J.R. Akridge, B. Schumm (Eds.), Proceedings of the Workshop on the Electrochemistry of Carbon, The Electrochemistry Society, Pennington, New Jersey, 1984, pp. 191–220.
[12] C. Lin, J.A. Ritter, B.N. Popov, J. Electrochem. Soc. 146 (1999) 3639.
[13] H.K. Song, H.Y. Hwang, K.H. Lee, L.H. Dao, Electrochim. Acta 45 (2000) 2241.
[14] P.L. Taberna, P. Simon, J.F. Fauvarque, J. Electrochem. Soc. 150 (2003) 292.
[15] C. Portet, P.L. Taberna, P. Simon, C. Laberty-Robert, Electrochim. Acta 49 (2004) 905.
[16] K.-L. Yang, S. Yiacoumi, C. Tsouris, J. Electroanal. Chem. 540 (2003) 159.